Cerebral Cortex April 2016;26:1365–1376
doi:10.1093/cercor/bhu225
Advance Access publication October 1, 2014

Synaptic Basis for Cross-modal Plasticity: Enhanced Supragranular Dendritic Spine Density in Anterior Ectosylvian Auditory Cortex of the Early Deaf Cat

H. Ruth Clemo[1], Stephen G. Lomber[2] and M. Alex Meredith[1]

[1]Department of Anatomy and Neurobiology, Virginia Commonwealth University School of Medicine, Richmond, VA 23298-0709, USA and [2]Brain and Mind Institute, National Centre for Audiology, University of Western Ontario, London, ON, Canada

Address correspondence to H. Ruth Clemo, PhD, Department of Anatomy and Neurobiology, Virginia Commonwealth University School of Medicine, 1101 E. Marshall Street, Sanger Hall Room 12-017, Richmond, VA 23298-0709, USA. Email: rclemo@vcu.edu

In the cat, the auditory field of the anterior ectosylvian sulcus (FAES) is sensitive to auditory cues and its deactivation leads to orienting deficits toward acoustic, but not visual, stimuli. However, in early deaf cats, FAES activity shifts to the visual modality and its deactivation blocks orienting toward visual stimuli. Thus, as in other auditory cortices, hearing loss leads to cross-modal plasticity in the FAES. However, the synaptic basis for cross-modal plasticity is unknown. Therefore, the present study examined the effect of early deafness on the density, distribution, and size of dendritic spines in the FAES. Young cats were ototoxically deafened and raised until adulthood when they (and hearing controls) were euthanized, the cortex stained using Golgi-Cox, and FAES neurons examined using light microscopy. FAES dendritic spine density averaged 0.85 spines/μm in hearing animals, but was significantly higher (0.95 spines/μm) in the early deaf. Size distributions and increased spine density were evident specifically on apical dendrites of supragranular neurons. In separate tracer experiments, cross-modal cortical projections were shown to terminate predominantly within the supragranular layers of the FAES. This distributional correspondence between projection terminals and dendritic spine changes indicates that cross-modal plasticity is synaptically based within the supragranular layers of the early deaf FAES.

Keywords: auditory, hearing loss, somatosensory, synaptic plasticity, visual

Introduction

The loss of a major sensory system (e.g., vision and hearing) during development leads to its neural replacement by the remaining sensory systems through a process termed "cross-modal plasticity." Indeed, in early deaf humans, brain imaging studies have revealed areas of auditory cortex activated by simple visual (Hickok et al. 1997; Finney et al. 2001) or tactile (Auer et al. 2007) stimuli, lip reading (Nishimura et al. 1999; Petitto et al. 2000), and even sign language (Cardin et al. 2013). Although it has often been proposed that these cross-modal effects are based on the neuroplastic properties of the brain (Rauschecker 1995; Bavelier and Neville 2002; Roder and Rosler 2004; Kral and Eggermont 2007; Merabet and Pascual-Leone 2010), the actual mechanisms for this plasticity are unknown, being largely inaccessible for study in human subjects. On the other hand, studies in experimental animals have not only revealed cross-modal effects (Hunt et al. 2006; Lomber et al. 2010, 2011; Meredith and Lomber 2011; Meredith et al. 2011; Meredith and Allman 2012), but also have begun to elucidate the neuronal basis for deafness-induced cross-modal plasticity. Recent single-unit recording studies have reported visual (and somatosensory) responses in auditory cortical areas of early deaf animals [cat: anterior auditory field (AAF; Meredith and Lomber 2011); auditory field of the anterior ectosylvian sulcus FAES (Meredith et al. 2011); ferret: AAF/A1 (Meredith and Allman 2012)], where those same modalities have a minor presence in hearing controls (Kayser et al. 2008; Bizley and King 2009; Mao et al. 2011; Meredith et al. 2012). Using anatomical tracers, several recent studies have examined projections to cross-modally reorganized areas in deaf cats (Barone et al. 2013; Chabot et al. 2013; Kok et al. 2014; Meredith et al. 2013) and ferrets (Allman et al. 2009; Meredith and Allman 2012), and observed that the connections in the deaf closely resembled those found in hearing animals. Hence, these recent anatomical findings demonstrate that cross-modal plasticity is not dependent on novel projections from non-auditory regions, but instead must largely result from the reweighting of existing connections.

For reweighting of existing inputs to occur, the relevant locus of plasticity most likely resides at the axon terminal, where the afferent axons synapse to excite post-synaptic neurons within the auditory cortex. There, excitatory cortical inputs to principal (pyramidal) cortical neurons, are known to synapse primarily on dendritic spines. Dendritic spines vary in shape, and those that occur as straight (sessel) or expanded (pedunculated) extension of dendritic membrane that generally represents mature, stable synapses (Stuart et al. 2008). They also vary with location, being sparse near the soma and increasing in density on distal dendrites (Stuart et al. 2008). The density of dendritic spines varies by dendritic branch order (Jacobs et al. 2009), by cortical lamina (Foxworthy et al. 2013), by cortical region (e.g., Clemo and Meredith 2012), and also by regional hierarchy (Jacobs et al. 2009). Spine numbers have been shown to be affected by a host of genetic, environmental, and pharmacological factors. For example, individuals with trisomy-21 (Purpura 1974), fragile-X syndrome (Comery et al. 1997), or schizophrenia (Garey et al. 1998) exhibit reduced spine densities, and stress (Bose et al. 2010), alcohol (Berman et al. 1996), or heroin exposure (Mei et al. 2009) also act to reduce spine numbers. On the other hand, environmental enrichment (Kolb et al. 2008) and exercise (Stranahan et al. 2007) enhance spine density values. In addition, dendritic spine density is significantly impacted by *intra*modal sensory deprivation, where neonatal deafening in rats (McMullen and Glaser 1988), visual deprivation in mice (Valverde 1967), and postnatal whisker trimming in mice (Briner et al. 2010), all result in decrements in spine density of neurons in the corresponding primary sensory cortices.

Dendritic spine size and stability are also parameters that are dynamically related to features of activity-dependent plasticity (Holtmaat et al. 2006). In fact, dendritic spine size is highly correlated with stability, where smaller spines are associated with immaturity and plasticity, while larger spines correspond with stable, mature neural circuits (Trachtenberg et al. 2002;

Kasai et al. 2003). Furthermore, activation that induces long-term potentiation (LTP) mediates effects that induce spine enlargement (Matsuzaki et al. 2004; Kasai et al. 2010) while those that induce long-term depression lead to spine shrinkage and retraction (Okamoto et al. 2004). Thus, dendritic spines are robust and well-studied indicators of excitatory synapse location and number, as well as neuronal circuit plasticity incurred under a variety of conditions. However, it is unknown whether dendritic spine density or distribution is affected by (or underlies) cross-modal plasticity.

Areas in which deafness-induced cross-modal plasticity has been demonstrated in experimental animals include: mouse: auditory cortex (Hunt et al. 2006), ferret: core auditory cortices AAF/A1 (Meredith and Allman 2012), cat: AAF (Meredith and Lomber 2011), auditory dorsal zone (DZ) (Lomber et al. 2010, 2011), posterior auditory field (Lomber et al. 2010, 2011), and FAES (Meredith et al. 2011). Although it has been sought, such plasticity has not been observed in cat primary auditory region A1 (Stewart and Starr 1970; Kral et al. 2003). The cortical sources of cross-modal afferents have been identified for ferret AAF/A1 (Meredith and Allman 2012—which evaluated thalamic connections as well), and for cat areas DZ (Kok et al. 2014), AAF (Chabot et al. 2013), and FAES (Meredith et al. 2013). It has also been shown in cats that early deafness alters the cartography of the auditory cortical regions, as indicated by shifts in cytoarchitectonic staining (Wong et al. 2014). While auditory activity strongly predominates in these regions in hearing animals (Meredith and Clemo 1989; Clarey and Irvine 1990a; Clemo et al. 2007), single-unit recordings in early deafened cat AAF or FAES revealed vigorous visual and somatosensory activities that were characterized by receptive field properties that were consistent with those of higher-level sensory cortices (Meredith and Lomber 2011; Meredith et al. 2011). In addition, approximately 70% of FAES activity was visually driven in early deaf cats and its reversible deactivation blocked visual orienting behaviors (Meredith et al. 2011). These studies indicate that, of all the cortical regions that have been demonstrated to be cross-modally reorganized by early deafening, the FAES is the most extensively characterized. Consequently, the present experiment was designed to examine the FAES of early deafened cats to determine the influence of cross-modal plasticity on the density and distribution of dendritic spines and to assess whether these effects correlated with the distribution of cross-modal afferent inputs to the region. The location of the FAES on a lateral view of the brain and a coronal cross-section is shown in Figure 1. An abstract of a preliminary version of this work has been presented (Clemo et al. 2013).

Materials and Methods

FAES Dendritic Spine Density

Tissue was derived from adult domestic cats involved with ongoing electrophysiological studies at the University of Western Ontario. Therefore, all procedures were conducted in accordance with the National Research Council's *Guidelines for the Care and Use of Mammals in Neuroscience and Behavioral Research* (2003), the Canadian Council on Animal Care's *Guide to the Care and Use of Experimental Animals* (Olfert et al. 1993), and were approved by the University of Western Ontario Animal Use Subcommittee of the University Council on Animal Care. Detailed descriptions of these other methodological procedures have been published (Carrasco and Lomber 2011). Three mature (>6M, 180 days postnatal is auditory maturity for cats; Kral et al. 2005) hearing (H) cats constituted the control group. Three mature (>6M) cats that were ototoxically deafened postnatally near the time of hearing onset (<1M) formed the early deaf group (D). This time frame was necessary because ototoxic procedures are maximally effective only after full hearing onset (~15 days postnatal; Xu et al. 1993), but treatment occurred well before the start of the auditory critical period for cats (~50 days postnatal; Kral et al. 2005). Deafness in all cases was confirmed by the absence of stimulus-evoked activity in an auditory brainstem response, as documented in other studies from this laboratory (Kok et al. 2014; Wong et al. 2014). Following the final experiment, animals were deeply anesthetized using sodium pentobarbital (40 mg/kg, i.v.), perfused through the ascending aorta with physiological saline followed by fixative (4% paraformaldehyde). All solutions were buffered to pH 7.4 with 0.1 M Sorenson's buffer and infused at a rate of 100 mL/min. The brain was then stereotaxically blocked in the coronal plane, removed from the skull, and immersed in 0.1 M phosphate buffer, and the non-recorded, intact, hemisphere was refrigerator-shipped to the Virginia Commonwealth University (VCU) for processing.

Golgi-Cox Staining

For Golgi-Cox staining, the cortex containing the auditory fields was processed over a proscribed period of 24 days using a Rapid GolgiStain Kit (FD NeuroTechnologies, Ellicott City, MD, USA). Following the incubation series, the blocks were sectioned serially (125 µm thickness) on a vibratome, mounted on gelatin-coated glass slides, and coverslipped using permount.

Data Collection

Golgi-Cox-prepared tissue sections containing the FAES were examined using low-magnification light microscopy to identify candidate cortical principal (pyramidal) neurons for evaluation. Specifically, stained pyramidal neurons were sought that demonstrated an identifiable soma with intact apical and basilar dendrites exhibiting dendritic spines. Once a neuron was selected, the entire section was traced and neuron was reconstructed using a Neuroludica (MBF MicroBrightfield, Inc., Willston, VT, USA) light-microscopic system. Candidate portions of apical (extending from the apex of soma toward the pial surface) and basilar (extending approximately horizontally from the base of the neuron) dendrites were selected and, using high magnification (×1000, oil), the location of each visible dendritic spine was marked. Both sessile and pedunculated dendritic spines were identified [according to the criteria of Stuart et al. (2008)] and marked. Filopodic spines were not marked because these were considered immature and often lack functional or mature synaptic contacts (Stuart et al. 2008). In addition, because spine densities diminish at locations close to the neuronal soma, no spines were evaluated <100 µm from the soma (Elston 2000). As a consequence, spines were largely derived from secondary and tertiary dendritic branches and only if the dendritic segment could be followed for >40 µm. This process was repeated until at least 1 apical and 2–4 basilar dendrites were examined for each of 20–25 FAES neurons from each case ($n = 3$ early deaf and 3 hearing). Each neuron was evaluated and recorded only by its slide and case number, meaning that the rater was blinded from treatment designations (hearing vs. early deaf) during data collection.

Data Analysis

Plots of dendritic segments marked with dendritic spines were analyzed using the NeuroExplorer (MBF MicroBrightfield, Inc.) software which determined the length of dendrite measured and counted the number of spines marked along that segment. These values were used to calculate spine density (spines/µm), which was tabulated according to treatment (hearing control or early deaf), laminar location of the parent neuron (supragranular = cortical layers 1, 2, and 3; infragranular = cortical layers 5 and 6; pyramidal neurons were not observed in the granular layer 4), dendritic location (apical and basilar), and branch order. Statistical methods were used to determine the average, and standard error of the mean, of spine densities according to the different variables. To evaluate dendritic spine size, dendrites were visualized using high-power (×100 objective oil) light microscopy. A segment (20–25 µm length) of dendrite (branch orders 2–5 only) was selected, along which each dendritic spine connected to it was sequentially examined. Once a selected

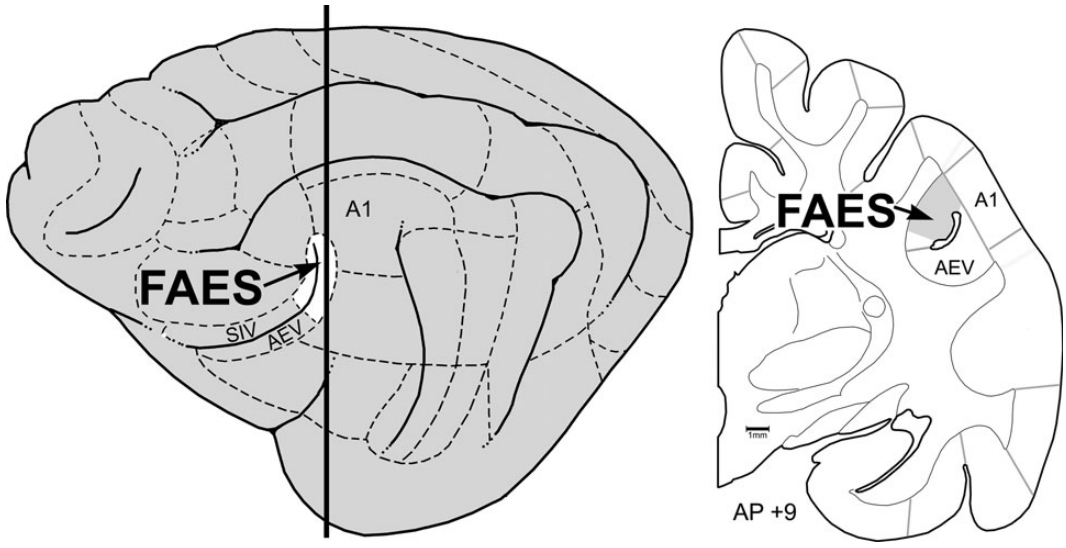

Figure 1. Location of the auditory FAES. The lateral view of the cat cortex (left) shows the location of the anterior ectosylvian sulcus, depicted as opened to expose its dorsal and ventral banks. The posterior banks (white, at arrow) contain the auditory representation of the FAES, whereas the anterior-dorsal bank contains the SIV and the anterior-ventral bank contains the AEV. Dashed lines indicate functional subdivisions of the cortex, where primary auditory cortex (A1) is labeled as a point of reference. The thick vertical line indicates the approximate anterior–posterior (AP) level from which the coronal section (right; ~AP + 9) was taken. Here, the anterior ectosylvian sulcus resides deep to the middle ectosylvian gyrus (labeled A1) and contains the FAES (at arrow). Gray lines depict the functional subdivisions of the cortex; the grayed-area of the coronal section represents the smaller representation of the FAES region in early deaf cats (after Wong et al. 2014).

spine was in focus, the NeuroLucida Quick-measure line tool was placed over the image of the spine head and its diameter was measured at its widest dimension and recorded. This procedure was repeated for every clearly visible dendritic spine along a selected dendrite. Three to 5 dendritic segments were sampled from each neuron from 3 to 5 neurons per animal. All data were tabulated and stored in a spreadsheet for subsequent analysis. All data were examined for normalcy of distribution using a Shapiro–Wilkes test; normally distributed sets were compared using a *t*-test, whereas non-normally distributed data sets were compared using a Wilcoxon rank sum test, and data across multiple groups were compared using ANOVA with post hoc Tukey's tests ($P < 0.05$ = significant; JMP Statistical Discovery Software, SAS Institute, Inc., Cary, NC, USA). Representative neurons were reconstructed using camera lucida (Nikon Eclipse 400 with Y-ITD attachment) and associated dendritic segments were photographed (Nikon Eclipse 60) and cropped using Photoshop (Adobe Systems) for graphic manipulation and display.

Laminar Distribution of Cross-modal Cortical Inputs to the FAES

Cortical Connectivity

Tissue was derived from adult domestic cats ($n = 9$) treated at VCU. Accordingly, all procedures were performed in compliance with the *Guide for Care and Use of Laboratory Animals* (NIH publication 86-23) and the National Research Council's *Guidelines for Care and Use of Mammals in Neuroscience and* Behavioral Research (2003) and approved by the Institutional Animal Care and Use Committee at VCU. Most procedures are described in detail in Dehner et al. (2004) and are largely summarized here.

Surgery and Tracer Injection

Mature, hearing cats were anesthetized with sodium pentobarbital (25 mg/kg. i.v.) and their heads secured in a stereotaxic frame. Under aseptic surgical conditions, a craniotomy was performed to expose the desired sensory cortical area. The latter were selected on the basis of preliminary connectional data for the FAES (Meredith et al. 2013) that demonstrate cortical projections to the region. The strongest include somatosensory projections from the AES, auditory projections from the AAF, and visual projections from the ectosylvian visual area (AEV) and lateral suprasylvian areas. However, because the AEV lies on the inferior border of the FAES, it is extremely difficult to inject tracer into the AEV without direct or indirect label contamination into the FAES. Accordingly, tracer injections targeted the fourth somatosensory area (SIV; Clemo and Stein 1982, 1983; $n = 4$) at approximately anterior–posterior (AP) +12 to +14 (Reinoso-Suárez 1961) or the visual postero-lateral lateral suprasylvian visual area (PLLS; Palmer et al. 1978; $n = 2$) at approximately AP +3 to +5 (Reinoso-Suárez 1961) and the AAF (Lee and Winer 2008b; $n = 3$) at approximately AP +11 to +12. Due to normal variability in gyral and sulcal features, cortical landmarks were used to guide final tracer injection placement into the selected area, where biotinylated dextran amine (BDA; 10 000 MW; lysine fixable; 10% in 0.1 M phosphate buffer) was pressure-injected (volume = ~1 µL). For each animal, only one site was injected and only one injection was made per site where the tracer deposit targeted all cortical layers. Subsequently, the cortex was covered with gel foam, the skin around the wound sutured closed, and standard postoperative care was provided. Results from each of these procedures have been reported for cortical areas other than the FAES (Clemo et al. 2007, 2008).

Histological Processing

Following a 7- to 10-day post-injection survival period, animals were euthanized (sodium pentobarbital, 50 mg/kg, i.p.) and perfused intracardially with saline followed by fixative (4.0% paraformaldehyde). The brain was blocked stereotaxically in the coronal plane, removed, and cryoprotected. Sections (50 µm thick) were cut serially using a freezing microtome. A series of sections (~300 µm intervals) was processed for visualization of BDA using the avidin–biotin peroxidase method using nickel–cobalt intensification. Reacted sections were mounted on gelatin-coated glass slides and coverslipped without counterstain.

Data Analysis

To assess the termination of projections from various sensory cortices into the FAES, the BDA labeling of axon terminals was digitally plotted using a light microscope (Nikon Optiphot-2) coupled with a PC-driven digitizing stage controlled by the Neurolucida software (MBF Biosciences). For each selected tissue section, a calibrated tracing of the outline, the border between gray and white matter, the position of layer 4, and the positions of labeled axon terminals were produced. BDA-labeled axon terminals appeared as sharp, black swellings at the end of thin axon stalks or as symmetrical varicosities along the course

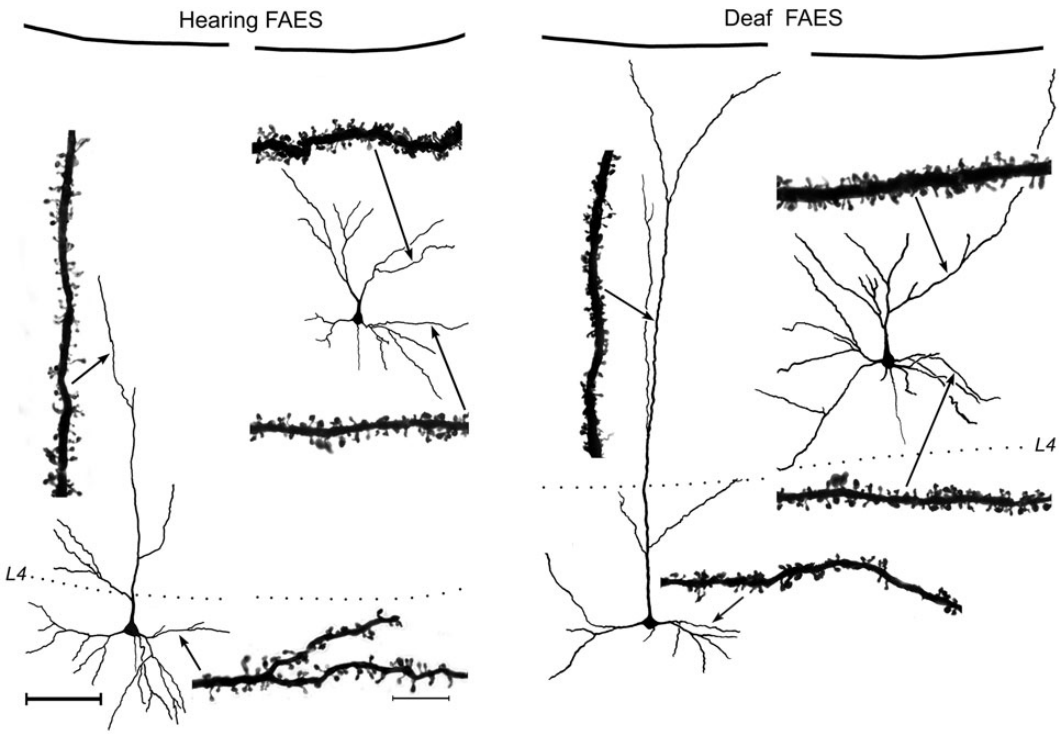

Figure 2. Golgi-stained pyramidal neurons from hearing (left) and early deaf (right) FAES are reconstructed relative to supragranular or infragranular laminar location (pia = top; dotted line = granular layer L4) using camera lucida. Photomicrographs (×1000, oil) depict the dendritic spines of selected examples of apical and basilar dendrites at sites indicated by the arrows. Scale bars for the neurons and dendrites are shown in the left panel: neuron scale bar (left) = 100 μm; dendritic segment scale bar = 10 μm.

of an axon. The Neurolucida software kept a count of the number of identified boutons. To determine the laminar distribution of labeled boutons, the NeuroExplorer program (MBF Biosciences) counted the number of marked axon terminals above (supragranular) and below (infragranular) layer 4. For each section, a ratio of labeled boutons in supragranular versus infragranular locations was determined and the mean was then calculated for all sections through the FAES for a given case.

Results

Dendritic Spine Density

A total of 154 Golgi-stained FAES neurons were examined (H = 73 and D = 81). Reconstructed examples of FAES neurons with cell bodies located in the supragranular or infragranular layers are depicted in Figure 2, where dendritic spines are visible at high magnification (×1000, oil) on their apical and basilar dendrites. A total of 1189 dendritic segments (H = 571 and D = 618) were measured on which 44 538 spines (H = 22 097 and D = 22 441) were counted (Table 1). Because spine density varies with the dendritic branch order, spine counts by branch order were compared between the hearing and early deaf groups, and the sampling distribution was found to be quite similar (Fig. 3). When the density of dendritic spines (spines/μm) was calculated, values from early deaf animals were normally distributed (Shapiro–Wilkes W test, $P = 0.159$), whereas those from hearing animals were significantly skewed toward the lower range (Shapiro–Wilkes W test, $P < 0.0079$). When compared, the average spine density for all measured FAES neurons from early deaf animals was found to be significantly higher (Wilcoxon; $P < 0.0001$) than that derived from the hearing controls [D avg. = 0.958 ± 0.011 standard error (SE); $n = 618$; H avg. = 0.858 ± 0.012 SE; $n = 571$], as illustrated in Figure 4*A*. From this figure, it can be seen that not only was there a trend for higher spine density values in the early deaf animals, but also the range of values was broader (D range = 0.23–2.13 spines/μm and H range = 0.31 –1.74 spines/μm). Furthermore, this enhancement of spine density was maintained across the dendritic branch order, as depicted in Figure 4*B*. For each branch order from the second to the sixth, dendritic spine densities were significantly (ANOVA; post hoc Tukey test, $P < 0.05$) higher in the early deaf, and the trend was maintained for values measured from seventh order

Table 1
Spine density of pyramidal neurons in the FAES

Dendrite type	Spine density
Hearing (n = 3; 73; 571; 22 097)	0.86 ± 0.01
All apical	0.91 ± 0.02
All basilar	0.83 ± 0.01
Supragranular	0.97 ± 0.02
Apical	1.03 ± 0.03
Basilar	0.95 ± 0.02
Infragranular	0.76 ± 0.01
Apical	0.82 ± 0.22
Basilar	0.72 ± 0.02
Deaf (n = 3; 81; 618; 22 441)	0.96 ± 0.01
All apical	1.10 ± 0.02
All basilar	0.88 ± 0.01
Supragranular	1.03 ± 0.01
Apical	1.12 ± 0.02
Basilar	0.96 ± 0.02
Infragranular	0.79 ± 0.02
Apical	0.89 ± 0.03
Basilar	0.73 ± 0.02

Note: n = number of cases; neurons; dendrites; spines. Spine density = mean ± SE.

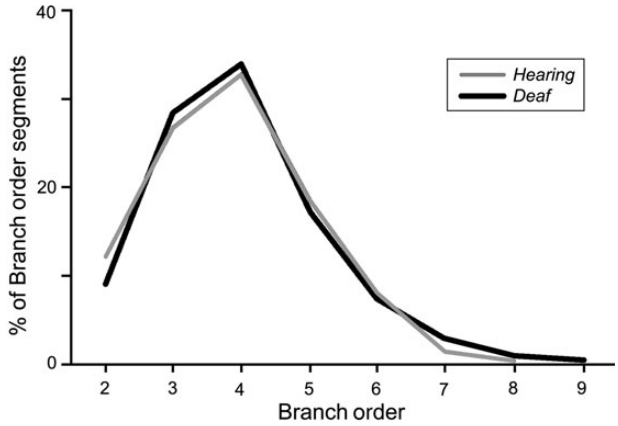

Figure 3. Measures of dendritic spine density (spines/μm) were acquired for the hearing and early deaf cats according to several variables, including the dendritic branch order. This graph indicates that dendritic branch orders 2–9 were systematically evaluated, and that the proportions of branch orders sampled were very similar between the hearing and early deaf conditions.

dendrites, although the sample size at this level was insufficient for statistical comparison. Due to the nature of the tissue preparation (125 μm thick sections), few labeled neurons retained intact dendritic branching beyond the eighth or ninth order; thus few were sampled. Also, by design, no primary dendrites (branch order = 1) were sampled in the present study, because spine density is affected by proximity to the parent soma (Jacobs et al. 2009).

Dendritic Type and Spine Density

For cortical pyramidal neurons, apical dendrites extend upward toward the pial surface, whereas basilar dendrites emanate from the base of the neuron and generally exhibit a horizontal distribution. For FAES neurons of hearing animals, apical dendrites were observed to exhibit higher spine densities (0.91 ± 0.02; mean ± SE) than did their basilar (0.83 ± 0.01) counterparts (Wilcoxon, $P < 0.0001$) and this distinction persisted within the early deaf group (apical = 1.1 ± 0.02 and basilar = 0.88 ± 0.01; *t*-test; $P < 0.0001$). These differences in spine density on apical versus basilar dendrites have also been observed for principal neurons in other sensory cortices (Clemo and Meredith 2012; Foxworthy et al. 2013). Furthermore, as depicted in Figure 5*A*, the enhancement of spine density in early deaf versus control FAES was maintained across both dendritic types (apical comparison: Wilcoxon, $P < 0.0001$; basilar comparison: Wilcoxon, $P < 0.032$).

Laminar Effects on Spine Density

Because the laminar location of a neuronal soma is known to correlate with dendritic spine density (e.g., Clemo and Meredith 2012; Foxworthy et al. 2013), the spine density values were compared for dendrites of supragranular and infragranular FAES neurons as summarized in Table 1. For neurons from hearing animals, spine densities were observed to be higher for supragranular (0.97 ± 0.02; mean ± SE) than infragranular neurons (0.76 ± 0.01; Wilcoxon, $P < 0.0001$), and this distinction persisted for neurons from the early deaf FAES (supragranular = 1.03 ± 0.01 and infragranular = 0.79 ± 0.02; *t*-test, $P < 0.0001$). However, when laminar effects were compared between the hearing and early deaf

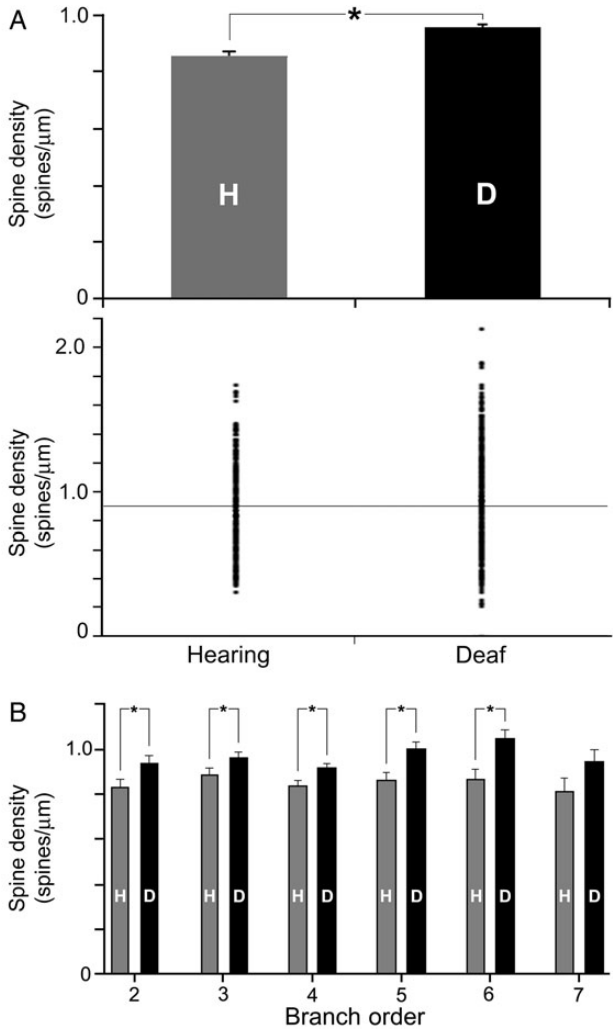

Figure 4. Dendritic spine density values are higher for FAES neurons in early deaf cats than from their hearing counterparts. (*A*) The bar graph (mean and SE) shows that the average dendritic spine density of FAES neurons was significantly (asterisk; *t*-test; $P < 0.0001$) higher for early deaf animals (D) than in the hearing (H) controls. The distribution plot (1 dot = value from 1 dendritic segment) also shows that early deaf animals had a broader range that was biased to higher levels than for the hearing controls. These same conventions are used in subsequent figures. (*B*) This elevated (mean and SE) spine density level in early deafened animals was observed consistently across the different dendritic branch orders, and was statistically significant (*t*-test, $P < 0.05$) for branch order segments 2–6.

neurons, as illustrated in Figure 5*B*, the enhanced spine density values for FAES neurons in early deaf animals were observed for only supragranular (Wilcoxon, $P < 0.012$), but not among infragranular, neurons.

Given that both laminar location and dendritic type appeared to influence spine density, additional analysis grouped spine density values by both parameters (Table 1), and compared them, as depicted in Figure 5*C*. For hearing animals, apical (1.03 ± 0.03) and basilar spine densities (0.95 ± 0.02) from supragranular neurons were significantly different (Wilcoxon, $P < 0.032$) as were apical (0.82 ± 0.22) and basilar (0.72 ± 0.02; Wilcoxon, $P < 0.005$) values for infragranular neurons. As expected, the same pattern persisted for measures from early deaf FAES, where apical (1.12 ± 0.02) and basilar spine densities (0.96 ± 0.02) from supragranular neurons were significantly different (Wilcoxon, $P < 0.0001$) as were apical (0.89 ± 0.03) and basilar (0.73 ± 0.02;

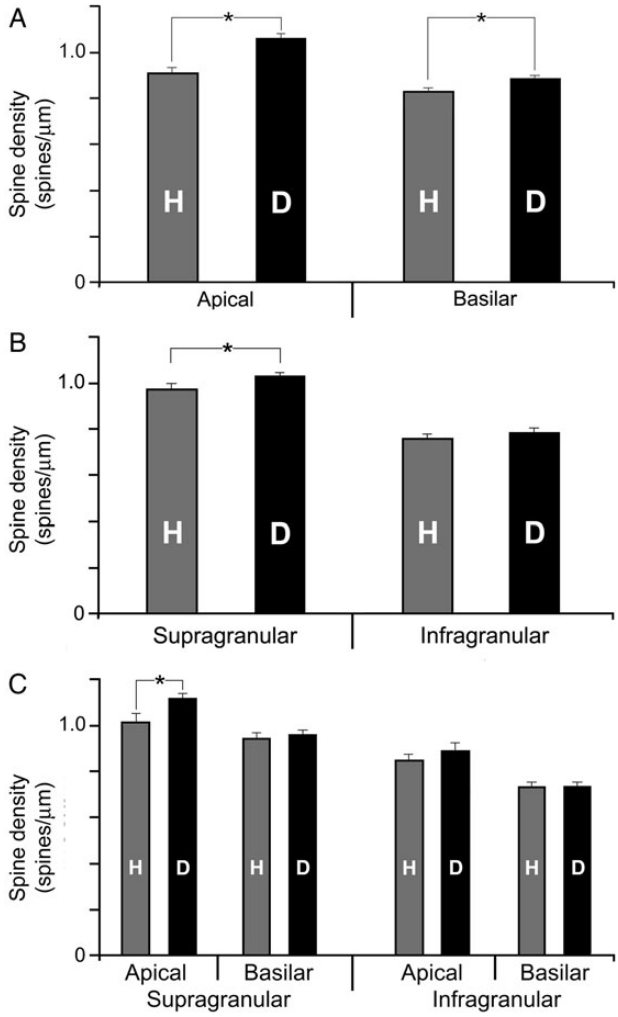

Figure 5. Only specific dendritic branches of FAES neurons from early deaf cats exhibit higher dendritic spine density than their hearing counterparts. (*A*) The bar graph shows that the average (±SE) dendritic spine density of apical or basilar dendritic segments was significantly higher ("asterisk," *t*-test, $P < 0.012$) in early deaf animals than in the hearing controls. In contrast, in (*B*), the bar graph (mean ± SE) shows that the average dendritic spine density of FAES neurons located in the supragranular layers was significantly higher (*t*-test, $P < 0.012$) in early deaf animals than in the hearing controls, but not in infragranular neurons. Furthermore, the bar graph (mean ± SE) in (*C*) divides the data into apical/basilar segments based on neuronal laminar location. When sorted by lamina, only apical dendrites of supragranular neurons showed a significant increase in spine density in early deaf animals. The other categories (supragranular–basilar segments; infragranular apical segments, and infragranular basilar segments) did not reveal significant alterations in spine density within the different treatment groups.

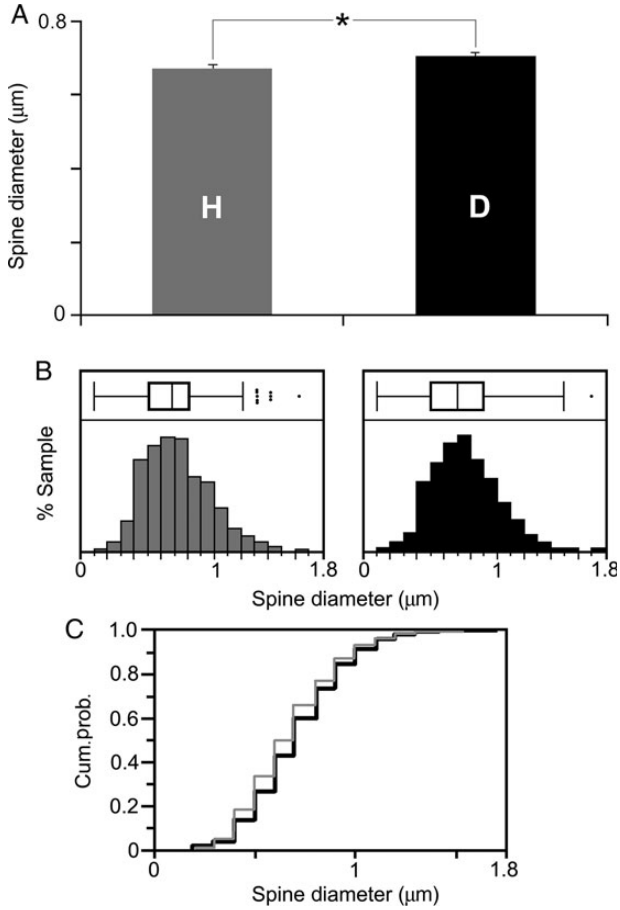

Figure 6. Dendritic spine head size (diameter) for hearing and early deaf FAES neurons. In (*A*), the average dendritic spine diameter from apical dendrites averaged 0.672 µm for hearing ("H"; gray bar: ±SE) and 0.707 µm for early deaf animals ("D"; black bar), which was statistically different (asterisk, Wilcoxon rank sum, $P < 0.001$). In (*B*), the distribution of spine head size is depicted for both the hearing (gray bars) and the early deaf (black bars) animals, where the range of dendritic spine sizes was essentially the same for both treatment groups. Box and whisker plots indicate 25–75% quartiles (box), mean (inside box-vertical line), range of sample (whiskers), and outliers (black dots). For hearing animals, the middle quartiles (25–75%) extended from 0.5 to 0.8, but for early deaf those same quartiles included spine measures from 0.5 to 0.9, indicating that proportionally more spines in the lower range were found in the hearing group. In (*C*), a cumulative probability distribution is shown for spine diameter values from hearing (gray line) and early deaf (black line) cases, where the lower spine measures (e.g., <0.8 µm) are consistently more prevalent in the hearing group.

t-test, $P < 0.0001$) values for infragranular neurons. However, as illustrated in Figure 5*C*, when the laminar/dendritic types were compared between hearing and deaf groups, only the apical dendrites of supragranular neurons from early deaf FAES revealed a significant (Wilcoxon, $P < 0.015$) change from the hearing controls.

Dendritic Spine Size

Given the established relationships between plasticity and spine size (e.g., Trachtenberg et al. 2002; Kasai et al. 2003), dendritic spine size also was measured and compared between hearing and early deaf conditions. Because significant spine density changes only were apparent for apical dendrites of supragranular FAES neurons (see above), the size of those same dendritic spines was measured. Defined as the widest dimension of the spine head, measures of spine head diameter were derived from a total of 928 dendritic spines from 54 apical dendritic segments of 13 neurons from the hearing animals and compared with 850 spines measured from 50 apical dendritic segments from 12 supragranular neurons from the early deaf cases. As shown in Figure 6*A*, the average diameter of dendritic spines in hearing FAES was 0.672 µm (±0.007 SE), whereas for the early deaf cases spine diameters averaged 0.707 µm (±0.008 SE) and ranged in size from 0.2 to 1.7 µm, as shown in Figure 5*B*. These values are similar to those observed for spine head diameter (avg. = 0.82 µm) and range (0.2–1.5 µm) for cortical pyramidal neurons in adult guinea pigs (Schüz 1986). Although the *range* of dendritic spine size was virtually the same for both groups, spine head diameters from the FAES

of hearing animals were significantly smaller (Wilcoxon rank sum; $z = 3.31$, $P < 0.0009$) than their counterparts in the early deaf FAES. In fact, proportionally fewer small spine heads (those <0.8 µm diameter) were observed in the early deaf than in the hearing FAES, as shown by the leftward shift in the box/whisker plot of spine head sizes from the hearing animals (Fig. 6*B*). This trend is also demonstrated in Figure 6*C*, where the cumulative frequency distribution of spine head measures from hearing animals consistently plotted toward the lower values, especially for spine diameter values between 0.4 and 0.8 µm in diameter.

Anterograde Labeling in the FAES

The above observations demonstrate that dendritic spine density is significantly enhanced specifically for apical dendrites of supragranular neurons in the cross-modally reorganized FAES. This raises the obvious question of why these particular dendrites were preferentially targeted. More specifically: What *prior* contacts might these particular dendrites have access to that would allow them to react in the observed manner? Because it is well established that there is a dynamic interaction between dendritic spines and the axon terminals that contact them, an additional series of experiments was included to examine the sources and distribution of afferent inputs to the FAES. By determining the laminar targets of such inputs, it is possible to evaluate whether there is a correspondence between established afferent inputs and the location of the dendritic spines that eventually exhibit cross-modal plasticity following deafness. Consequently, tracer injections of BDA were made into major sources of non-auditory input to the FAES (see Materials and Methods), including the visual posterolateral lateral suprasylvian area (PLLS; Palmer et al. 1978), the SIV (Clemo and Stein 1982, 1983; Meredith et al. 2006), and the AAF (Lee and Winer 2008a; Meredith et al. 2013). Inputs from each of these regions were labeled (individually) (PLLS $n = 2$; SIV $n = 4$; and AAF = 3) and their laminar distribution within the FAES was determined using a digitizing light-microscopic process (Neurolucida; MicroBrightField, Inc.). After tracer injection into the PLLS, labeled bouton terminals were identified at multiple A–P levels within the FAES, as depicted for the case illustrated in Figure 7. Counts of labeled boutons were made within the borders of the FAES and grouped according to their supra- or infragranular location (divided by a narrow layer 4). Analysis of these results showed that inputs from PLLS predominantly terminate (all cases, mean = 78% ± 10 SE) within the supragranular layers of the FAES. Similarly, a representative example of projections from somatosensory cortical area SIV is illustrated in Figure 8, where labeled axons preferentially (all cases, mean = 77% ± 2.3SE) terminated within the supragranular layers of the FAES. Finally, a representative example of projections from auditory cortical area AAF is depicted in Figure 9, where labeled boutons were found preferentially (all cases, mean = 88% ± 1.2 SE) within the supragranular layers of the FAES. These results show that auditory and non-auditory cortical inputs exhibit a prioritized access to the supragranular layers of the FAES and would, therefore, be present to

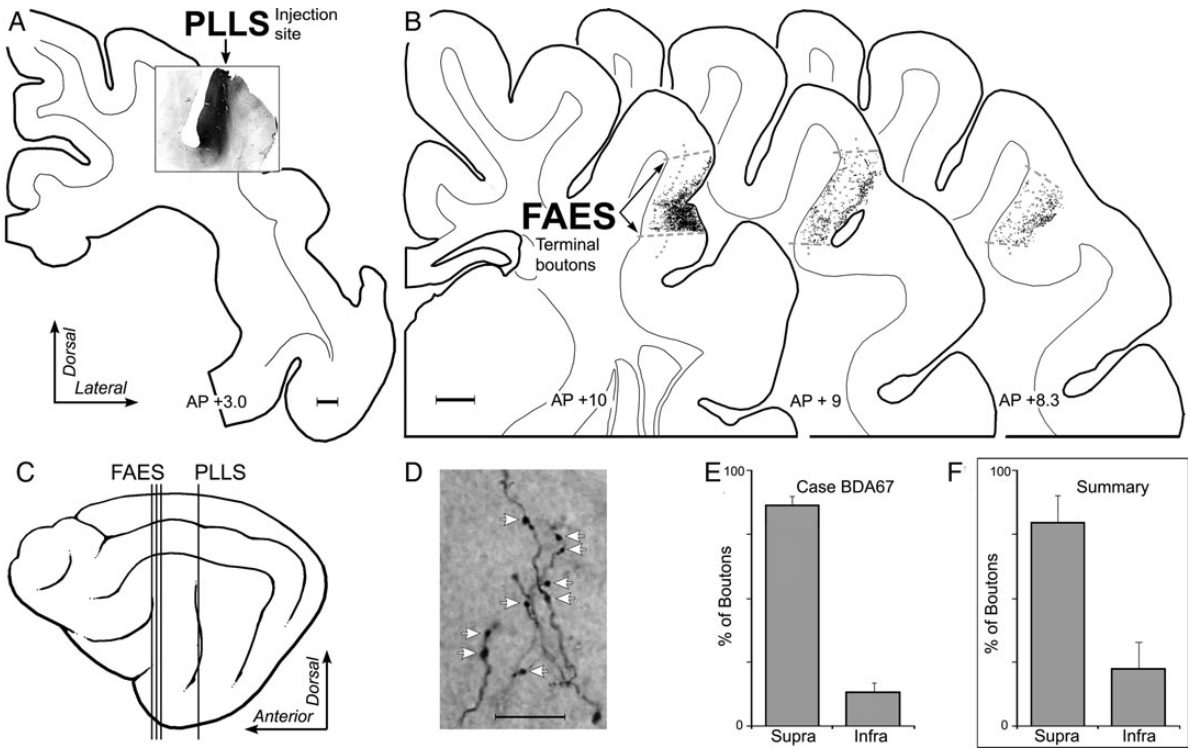

Figure 7. Laminar termination in the FAES of non-auditory inputs from visual PLLS. In (*A*), the coronal section shows the injection site (black area) in the lateral bank of the suprasylvian sulcus corresponding to the location of visual area PLLS (scale = 1 mm). In (*B*), coronal sections through the anterior (left), middle, and posterior (right) regions of the FAES (borders indicated by dashed gray lines; layer 4 indicated by dotted gray line) displaying terminal boutons (1 black dot = 1 bouton; scale = 1 mm) labeled from the PLLS injection site. The lateral view of cortex (*C*) illustrates the location (vertical lines) of the coronal sections through the PLLS (shown in *A*) and FAES (*B*). (*D*) is a micrograph (×1000, oil; scale = 10 µm) taken of representative PLLS-labeled axons and boutons (indicated at white arrows) within the FAES. When the number of boutons labeled from the PLLS were counted within the supragranular versus infragranular layers of the FAES for this case, the overwhelming proportion (mean = 86% ± 3 SE) was identified within supragranular layers, as quantitatively summarized in the bar graphs (*E*). Similarly, (*F*) the levels of boutons labeled from PLLS for all cases and sections predominantly (mean = 78% ± 10 SE) terminated within the supragranular layers of the FAES.

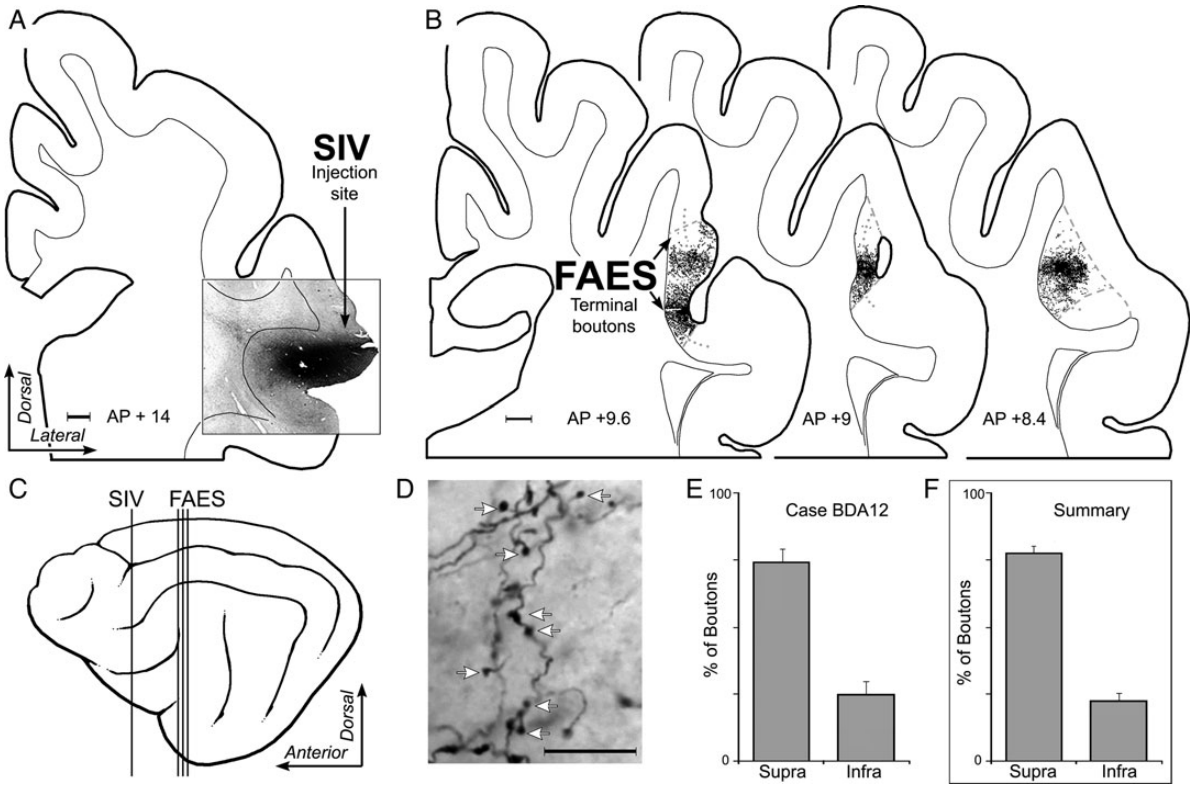

Figure 8. Laminar termination in the FAES of non-auditory inputs from the SIV. In (*A*), the coronal section shows the injection site (black area) in the dorsal bank of the anterior ectosylvian sulcus corresponding to the location of SIV (scale = 1 mm). (*B*) Coronal sections through the anterior (left), middle, and posterior (right) regions of the FAES (borders indicated by dashed gray lines; layer 4 indicated by dotted gray line) displaying terminal boutons (1 black dot = 1 bouton; scale = 1 mm) labeled from the SIV injection site. The lateral view of cortex (*C*) illustrates the location (vertical lines) of the coronal sections through the SIV (shown in *A*) and FAES (*B*). (*D*) is a micrograph (×1000, oil; scale = 10 μm) taken of representative SIV-labeled axons and boutons (indicated at white arrows) within the FAES. When the number of boutons labeled from the SIV were counted within the supragranular versus infragranular layers of the FAES for this case, the overwhelming proportion was identified within supragranular layers, as quantitatively summarized in *E* (mean = 75% ± 4.7 SE). Similarly, (*F*) the levels of boutons labeled from SIV for all cases and sections predominantly (mean = 77% ± 2.3 SE) terminated within the supragranular layers of the FAES.

contribute to the synaptic changes induced by deafness. Whether these same laminar preferences are maintained after deafness would be expected, since activity-dependent factors would favor their persistence.

Discussion

The auditory cortices of only a few species have been examined for their dendritic spine density. Adult values in area A1 in rat (avg. range = 1.05–1.65 spines/μm; Schachtele et al. 2011; avg. = 0.75 spines/μm, McMullen and Glaser 1988), ferret (avg. 1.27 ± 0.3 spines/μm; Clemo and Meredith 2012), and macaque (avg. = 0.74 ± 0.24 spines/μm; Elston et al. 2010) were within the range of that observed here for FAES neurons in hearing cats (overall avg. = 0.85 ± 0.01 spines/μm). Like other sensory cortices, the present study of FAES neurons showed that dendritic spine density also varied with a laminar, dendritic type and branch-order variables. However, the observation of increased spine density measures seen in the FAES following hearing loss appears to contradict the existing literature, where reductions in spine numbers after sensory deprivation were generally reported (Valverde 1967; McMullen and Glaser 1988; Briner et al. 2010). In particular, neonatal cochlear destruction was observed to reduce dendritic spine density in rat A1 from an average 0.75 (control) to 0.46 spines/μm (McMullen and Glaser 1988). These deafened A1 results were exclusively derived from laminar locations that correspond with the terminal zone of thalamic afferents from the medial geniculate nucleus, which were presumed to be reduced by the deafening procedure and A1 apical dendrites were not examined (McMullen and Glaser 1988). In contrast, the present study examined that the FAES, which is a higher-level auditory area distinct from A1, exhibits a different cytoarchitectural pattern characterized by reduced layer IV dimensions, and receives thalamic inputs from the medial and dorsal subdivisions (Lee and Winer 2008a) and non-specific subnuclei (suprageniculate, posterior and lateral-posterior; Clarey and Irvine 1990b). Because these non-specific thalamic regions receive their activation via long cortical loops (Sherman and Guillery 2011; Hackett 2012), they may not be as severely de-afferented in deafened subjects as those areas receiving the principle ascending auditory projection. Furthermore, A1 has not been demonstrated to exhibit cross-modal plasticity from deafness (Kral et al. 2003) that has been clearly observed in the FAES (Meredith et al. 2011, 2013). Therefore, it seems likely that regional differences can account for the discrepancies in spine density effects observed by these different studies.

The apical dendrites of supragranular FAES neurons not only revealed increased numbers (density) in the early deaf cats, but also exhibited significant changes (from hearing controls) in spine head diameter. Because larger spines correlate

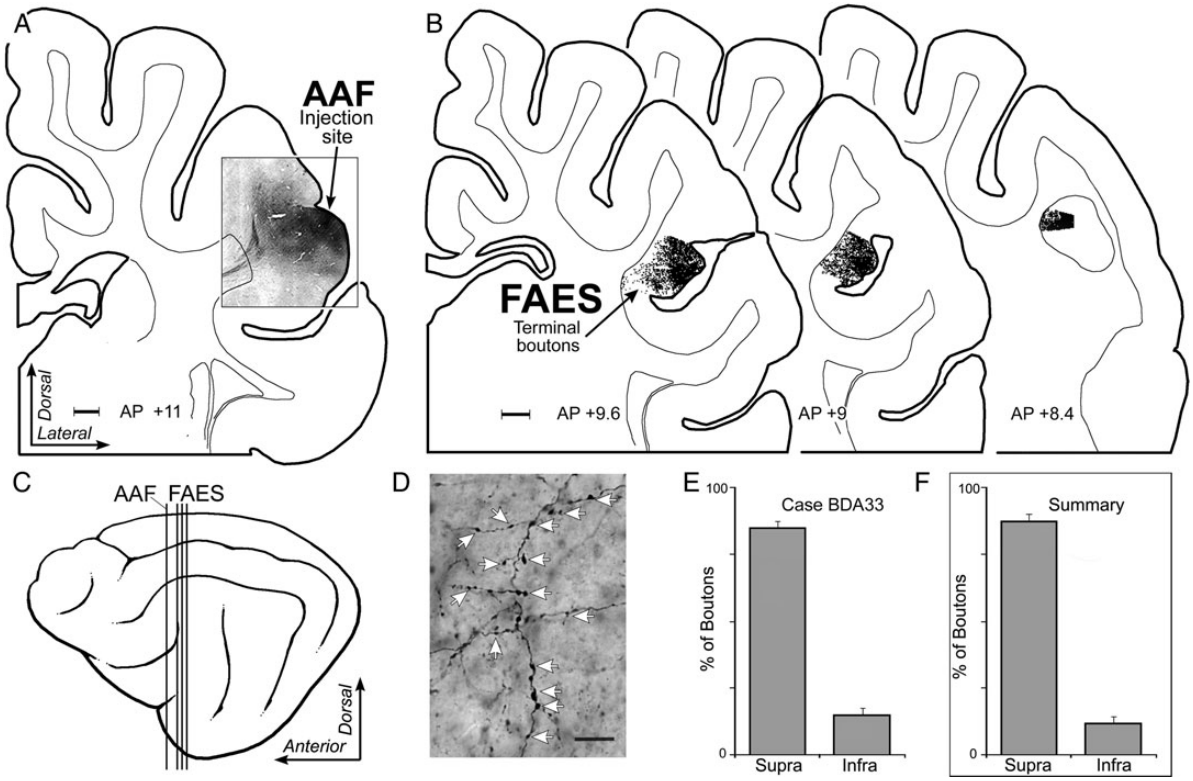

Figure 9. Laminar termination in the FAES of auditory inputs from AAF. In (*A*), the coronal section shows the injection site (black area) in the posterior portion of the anterior ectosylvian gyrus corresponding to the location of the gyral portion of the AAF (scale = 1 mm). (*B*) Coronal sections through the anterior (left), middle, and posterior (right) regions of the FAES displaying terminal boutons (1 black dot = 1 bouton; scale = 1 mm) labeled from the AAF injection site. The lateral view of cortex (*C*) illustrates the location (vertical lines) of the coronal sections through the AAF (shown in *A*) and FAES (*B*). (*D*) is a micrograph (×1000, oil; scale = 10 μm) taken of representative AAF-labeled axons and boutons (indicated at white arrows) within the FAES. When the number of boutons labeled from AAF were counted within the supragranular versus infragranular layers of the FAES for this case, the overwhelming proportion was identified within supragranular layers, as quantitatively summarized in *E* (mean = 85% ± 3 SE). Similarly, (*F*) the levels of boutons labeled from AAF for all cases predominantly (mean = 88% ± 1.2 SE) terminated within the supragranular layers of the FAES.

with stability, maturity (Trachtenberg et al. 2002; Kasai et al. 2003; Holtmaat et al. 2006), and even increased synaptic efficacy associated with LTP (Matsuzaki et al. 2004; Kasai et al. 2010), it would be tempting to suggest that cross-modal plasticity was achieved through the process of spine enlargement. However, it must be pointed out that the spines in early deaf animals exhibited the same range of dendritic spine head sizes that was obtained for hearing FAES. This observation is important, first, because it indicates that the excitatory synapses involved in signaling cross-modal messages in adult animals deafened in early life exhibit essentially the same stability and efficacy as synapses resulting from normal developmental conditions. Functionally, this is supported by the fact that cross-modal visual and/or somatosensory responses of FAES neurons have been demonstrated to be pervasive and vigorous in early deafened animals (Meredith et al. 2011). Furthermore, the present results indicate that the features of dendritic spine morphology that are associated with maintenance of cortical responsiveness following *intra*modal sensory deprivation (Lendvai et al. 2000; Oray et al. 2004; Kaneko et al. 2012) appear to apply to *cross*-modal effects as well. Secondly, the difference in spine head size was largely due to the presence of a higher proportion of smaller heads on FAES neurons of hearing animals. Given that spines with smaller diameters are associated with immaturity and/or plasticity (Trachtenberg et al. 2002; Kasai et al. 2003; Okamoto et al. 2004), these data suggest that cross-modally reorganized areas may lose some of their potential for continued plasticity which, itself, may be a consequence of the reduced input dimensionality of the deafened cortical region.

Dendritic Spine Plasticity

The present results indicate that cross-modal plasticity supports an increase in dendritic spine density in the early deaf FAES, and this effect was maintained across variables of lamina, dendrite location, and dendritic branch order. Because dendritic spines and synaptic boutons are both required components of a mature synapse, it should be expected that an increase in dendritic spines would be accompanied by a corresponding increase in presynaptic axon terminals. This specific information is not yet available. However, an indirect correlation was observed: non-auditory inputs to the FAES were found to preferentially target the same supragranular layers, where the principal changes in dendritic spine density were found. Given these observations and the well-known role of dendritic spines in synaptic plasticity (for review, see Holtmaat and Svoboda 2009; Segal 2010; Bosch and Hayashi 2012), activity-dependent mechanisms could readily promote the generation and maintenance of larger numbers of non-auditory connections in early deaf animals than would occur when in competition with auditory inputs. These factors would be predicted to result in non-auditory activation of supragranular FAES neurons in early deafened animals, whose activity could then spread to the other laminae via well-known

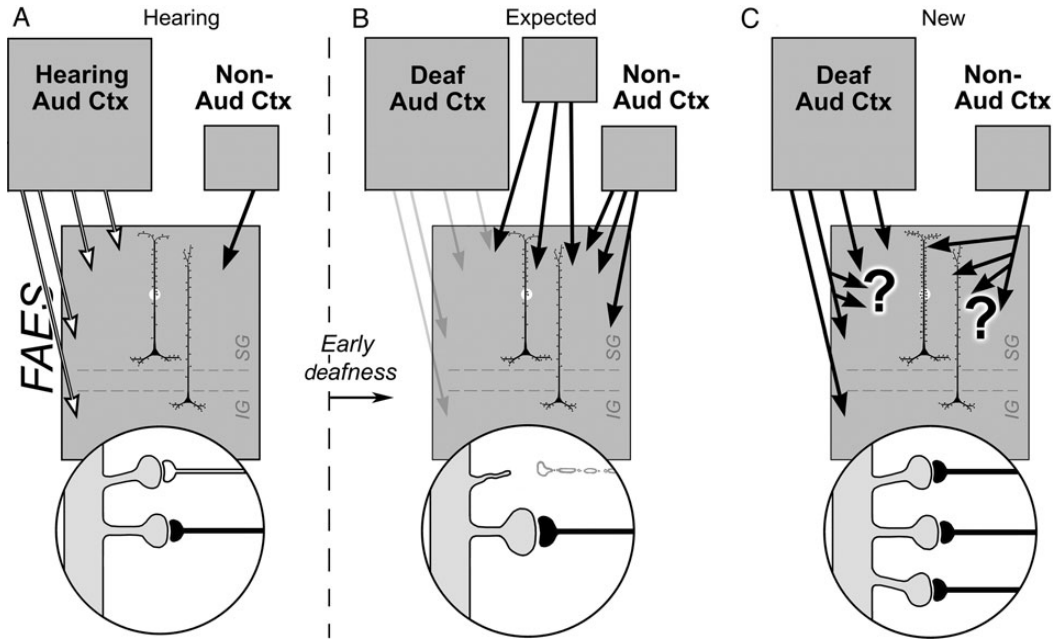

Figure 10. Summary of synaptic basis for deafness-induced cross-modal plasticity in the FAES. For hearing animals (*A*), neurons in the infraganular (IG) and supragranular (SG) laminae of the FAES (large gray box) predominantly receive inputs from auditory cortex (multiple white arrows) as well as a small projection from non-auditory cortical regions (black arrow). The highlighted segment of an FAES neuron's dendritic shaft is enlarged (bottom circle) to show spines with synaptic inputs from auditory cortex (white axon) as well as from non-auditory cortex (black axon). The schematics to the right of the vertical dashed line represent changes in the FAES induced by early deafness. (*B*) The historically expected effects of cross-modal plasticity represented by increases in inputs from new or existing non-auditory areas (black arrows) and/or by increased synaptic weighting/efficacy of existing non-auditory inputs (enlarged black axon and terminal). Although not explicitly stated, it has also been assumed that inputs from auditory cortex are lost/reduced after early deafness (retracted spine and white axon; faded arrows). In (*C*), recent data have observed that increased projections from new or existing non-auditory areas were not found, nor were connections with auditory cortex lost. In addition, dendritic spine numbers increased, without increases in spine size. These observations imply that increases in spine density may be paralleled by increases in afferent branching (large "?") and that most inputs to the FAES (from either auditory or non-auditory regions) now relay non-auditory signals (black axons).

local circuit projections and result in the generalized functional reorganization of the FAES described by Meredith et al. (2011).

Another possibility should be considered: Despite deafness and the ensuing lack of acoustically induced activity, inputs from auditory cortical regions are likely to continue to have access to the FAES. Although not considered by most models of deafness-induced cross-modal plasticity (Rauschecker 1995), recent connectional studies consistently report that auditory cortico-cortical projections remain connected to their cortical targets in early deafened animals (Meredith and Allman 2012; Barone et al. 2013; Chabot et al. 2013; Kok et al. 2014; Meredith et al. 2013). Under these circumstances, the established projections from AAF (Lee and Winer 2008a; present study) with the FAES would be expected to be maintained for the early deaf FAES. The nature of the signals these maintained (but deafened) connections might carry is currently unknown. A recent single-unit recording study has demonstrated that the early deaf AAF is cross-modally reorganized by visual and somatosensory responses (Meredith and Lomber 2011) and auditory area A2 shows cross-modal reorganization in early deaf humans (Hickok et al. 1997). Since both AAF and A2 are sources of inputs to the FAES (Lee and Winer 2008b), it seems possible that connections from these cortical regions in the early deaf convey visual and somatosensory signals to the FAES.

Cross-modal Mechanisms

The present results indicate that non-auditory inputs preferentially terminate in the supragranular layers of the FAES in hearing animals, as represented in Figure 10*A*. In contrast, early deaf animals exhibit a high proportion of non-auditory responses in the FAES (68% visual and 33% somatosensory; Meredith et al. 2011), although the mechanism for this neural reorganization has not been empirically established. Historically (Rauschecker 1995), cross-modal effects (meaning the replacement of auditory with non-auditory activity) in the early deaf have been explained as in-growth of non-auditory afferents from novel or existing loci, as depicted in Figure 10*B*, or by the reweighting of existing silent inputs (not depicted). However, neither mechanism can account for several recent observations. Specifically, both auditory and non-auditory projections to the deafened auditory cortices are essentially the same as those for hearing animals (Barone et al. 2013; Chabot et al. 2013; Kok et al. 2014; Meredith et al. 2013), meaning that new cortical sources essentially are not recruited from distant locations to functionally reorganize the "vacated" regions. A similar retention of connectivity was also observed for projections to cross-modally reorganized auditory cortical regions of the early deaf ferret (Meredith and Allman 2012). Although these data collectively indicate that cross-modal plasticity is not subserved by new connections from non-auditory sources, the notion that cross-modal plasticity results from unmasking of silent inputs also seems unlikely, since several studies have now demonstrated the presence of non-auditory activity in auditory cortex in hearing animals (Bizley and King 2009; Mao et al. 2011; Meredith et al. 2012). In contrast, the present study suggests an alternative mechanism for cross-modal plasticity in the early deaf FAES, as illustrated in Figure 10*C*. First, non-auditory signals arrive from

other, now reorganized auditory cortices along their maintained connections, as described above. Secondly, all inputs to the early deaf FAES (from both traditional auditory cortex and non-auditory sources) may exhibit higher levels of terminal branching to correspond with increased dendritic spine density, as illustrated in Figure 10*C*. Although increased spine/synapse density does not rule out the possibility that some existing, non-auditory synapses also become reweighted, it does offer empirical evidence for a new synaptically based, activity-dependent mechanism for cross-modal plasticity.

Conclusions

In summary, the present results demonstrate that, in the FAES region of cat auditory cortex, cross-modal plasticity induced by early deafness generates an increase in dendritic spine density, particularly on the apical dendrites of supragranular layer neurons. These laminar-based changes in post-synaptic dendritic elements correspond with the supragranular targeting preferences of cross-modal (presynaptic) inputs to the region, suggesting the participation of both elements of the synapse in this form of neuronal plasticity. Taken together, these observations provide some of the first empirical insights into neuronal and synaptic mechanisms underlying deafness-induced cross-modal plasticity.

Funding

This works was supported by Virginia Commonwealth University Presidential Research Quest Fund (M.A.M.) and the Canadian Institutes of Health Research (S.G.L.).

Notes

Conflict of Interest: None declared.

References

Allman BL, Keniston LP, Meredith MA. 2009. Adult-deafness induces somatosensory conversion of ferret auditory cortex. Proc Natl Acad Sci USA. 106:5925–5930.

Auer ET Jr, Bernstein LE, Sunkarat W, Singh M. 2007. Vibrotactile activation of the auditory cortices in deaf versus hearing adults. Neuroreport. 18:645–648.

Barone P, Lacassagne L, Kral A. 2013. Reorganization of the connectivity of cortical field DZ in congenitally deaf cat. PLoS ONE. 8: e60093.

Bavelier D, Neville HJ. 2002. Cross-modal plasticity: where and how? Nat Rev Neurosci. 3:443–452.

Berman RF, Hannigan JH, Sperry MA, Zajac CS. 1996. Prenatal alcohol exposure and the effects of environment on hippocampal dendritic spine density. Alcohol. 13:209–216.

Bizley JK, King AJ. 2009. Visual influences on ferret auditory cortex. Hear Res. 258:55–63.

Bosch M, Hayashi Y. 2012. Structural plasticity of dendritic spines. Curr Opin Neurobiol. 22:383–388.

Bose M, Munoz-Llanco P, Roychowdhury S, Nichols JA, Jakkamsetti V, Porter B, Byrapureddy R, Salgado H, Kilgard MP, Aboitiz F et al. 2010. Effect of the environment on the dendritic morphology of the rat auditory cortex. Synapse. 64:97–110.

Briner A, DeRoo M, Dayer A, Muller D, Kiss JZ, Vutskits L. 2010. Bilateral whisker trimming during early postnatal life impairs dendritic spine development in the mouse somatosensory barrel cortex. J Comp Neurol. 518:1711–1723.

Cardin V, Orfanidou E, Rönnberg J, Capek CM, Rudner M, Woll B. 2013. Dissociating cognitive and sensory neural plasticity in human superior temporal cortex. Nat Commun. 4:1473.

Carrasco A, Lomber SG. 2011. Neuronal activation times to simple, complex, and natural sounds in cat primary and nonprimary auditory cortex. J Neurophysiol. 106:1166–1178.

Chabot N, Kok M, Lomber SG. 2013. Amplified somatosensory and visual cortical projections underlie cross modal plasticity in the anterior auditory field of early deaf. Soc Neurosci Abstr. 43:455.07.

Clarey JC, Irvine DRF. 1990a. The anterior ectosylvian sulcal auditory field in the cat: I. An electrophysiological study of its relationship to surrounding auditory cortical fields. J Comp Neurol. 301:289–303.

Clarey JC, Irvine DRF. 1990b. The anterior ectosylvian sulcal auditory field in the cat: II. A horseradish peroxidase study of its thalamic and cortical connections. J Comp Neurol. 301:304–324.

Clemo HR, Allman BL, Donlan MA, Meredith MA. 2007. Sensory and multisensory representations within the cat rostral suprasylvian cortices. J Comp Neurol. 503:110–127.

Clemo HR, Lomber SG, Meredith MA. Forthcoming 2013. Dendritic spine density is enhanced by deafness-induced crossmodal plasticity in the auditory field of the anterior ectosylvian sulcus (FAES). Soc Neurosci Abstr. 43:4170.

Clemo HR, Meredith MA. 2012. Dendritic spine density in differs in multisensory versus primary sensory cortex. Synapse. 66:714–724.

Clemo HR, Sharma GK, Allman BL, Meredith MA. 2008. Auditory projections to extrastriate visual cortex: connectional basis for multisensory processing in "unimodal" visual neurons. Exp Brain Res. 191:37–47.

Clemo HR, Stein BE. 1983. Organization of a fourth somatosensory area of cortex in cat. J Neurophysiol. 50:910–925.

Clemo HR, Stein BE. 1982. Somatosensory cortex: a "new" somatotopic representation. Brain Res. 235:162–168.

Comery TA, Haris JB, Willems PJ, Oostra BA, Irwin SA, Weiler IJ, Greenough WT. 1997. Abnormal dendritic spines in fragile X knockout mice: maturation and pruning effects. Proc Natl Acad Sci USA. 94:5401–5404.

Dehner LR, Clemo HR, Meredith MA. 2004. Cross-modal circuitry between auditory and somatosensory areas of the cat anterior ectosylvian sulcal cortex: a "new" form of multisensory convergence. Cereb Cortex. 14:387–401.

Elston GN. 2000. Pyramidal cells of the frontal lobe: all the more spinous to think with. J Neurosci. 20:RC95.

Elston GN, Okamoto T, Oga T, Dornan D, Fujita I. 2010. Spinogenesis and pruning in the primary auditory cortex of the macaque monkey (*Macaca fascicularis*): an intracellular injection study of layer III pyramidal cells. Brain Res. 1316:35–42.

Finney EM, Fine I, Dobkins KR. 2001. Visual stimuli activate auditory cortex in the deaf. Nat Neurosci. 4:1171–1173.

Foxworthy WA, Clemo HR, Meredith MA. 2013. Laminar and connectional organization of a multisensory cortex. J Comp Neurol. 521:1867–1890.

Garey LJ, Ong WY, Patel TS, Kanani M, Davis A, Mortimer AM, Barnes TRE, Hirsch SR. 1998. Reduced dendritic spine density on cerebral cortical pyramidal neurons in schizophrenia. J Neurol Neurosurg Psychiatry. 65:446–453.

Hackett TA. 2012. Multisensory convergence in the thalamus. In: Stein BE, editor. "The New Handbook of Multisensory Processing." Cambridge (MA): MIT Press. pp. 49–66.

Hickok G, Poeppel D, Clark K, Buxton RB, Rowley HA, Roberts TP. 1997. Sensory mapping in a congenitally deaf subject: MEG and fMRI studies of cross-modal non-plasticity. Hum Brain Mapp. 5:437–444.

Holtmaat A, Svoboda K. 2009. Experience-dependent structural synaptic plasticity in the mammalian brain. Nat Rev Neurosci. 10:647–658.

Holtmaat A, Wilbrecht L, Knott GW, Welker E, Svoboda K. 2006. Experience-dependent and cell-type-specific spine growth in the neocortex. Nature. 441:979–983.

Hunt DL, Yamoah EN, Krubitzer L. 2006. Multisensory plasticity in congenitally deaf mice: how are cortical areas functionally specified? Neuroscience. 139:1507–1524.

Jacobs B, Schall M, Prather M, Kapler E, Driscoll L, Baca S, Jacobs J, Ford K, Holtmaat A, Svoboda K. 2009. Experience-dependent

structural synaptic plasticity in the mammalian brain. Nat Rev Neurosci. 10:647–658.
Kaneko M, Xie Y, An JJ, Stryker MP, Xu B. 2012. Dendritic BDNF synthesis is required for late-phase spine maturation and recovery of cortical responses following sensory deprivation. J Neurosci. 32:4790–4802.
Kasai H, Hayama T, Ishikawa M, Watanabe S, Yagishita S, Noguchi J. 2010. Learning rules and persistence of dendritic spines. Eur J Neurosci. 32:241–249.
Kasai H, Matsuzaki M, Noguchi J, Yasumatsu N, Nakahara H. 2003. Structure-stability function relationships of dendritic spines. Trends Neurosci. 26:360–368.
Kayser C, Petkov CI, Logothetis NK. 2008. Visual modulation of neurons in auditory cortex. Cereb Cortex. 18:1560–1574.
Kok MA, Chabot N, Lomber SG. 2014. Cross-modal reorganization of cortical afferents to dorsal auditory cortex following early- and late-onset deafness. J Comp Neurol. 522:654–675.
Kolb B, Cioe J, Comeau W. 2008. Contrasting effects of motor and visual spatial learning tasks on dendritic arborization and spine density in rats. Neurobiol Learn Mem. 90:295–300.
Kral A, Eggermont JJ. 2007. What's to lose and what's to learn: development under auditory derivation, cochlear implants and limits of cortical plasticity. Brain Res Rev. 56:259–269.
Kral A, Schroder JH, Klinke R, Engel AK. 2003. Absence of cross-modal reorganization in the primary auditory cortex of congenitally deaf cats. Exp Brain Res. 153:605–613.
Kral A, Tillein J, Heid J, Hartmann R, Klinke R. 2005. Postnatal cortical development in congenital auditory deprivation. Cereb Cortex. 15:552–562.
Lee CC, Winer JA. 2008a. Connections of cat auditory cortex: I. Thalamocortical system. J Comp Neurol. 507:1879–1900.
Lee CC, Winer JA. 2008b. Connections of cat auditory cortex: III. Corticocortical system. J Comp Neurol. 507:1920–1943.
Lendvai B, Stern EA, Chen B, Svoboda K. 2000. Experience-dependent plasticity of dendritic spines in the developing rat barrel cortex in vivo. Nature. 404:876–881.
Lomber SG, Meredith MA, Kral A. 2011. Adaptive crossmodal plasticity in deaf auditory cortex: areal and laminar contributions to supranormal vision in the deaf. Prog Brain Res. 191:251–270.
Lomber SG, Meredith MA, Kral A. 2010. Crossmodal plasticity in specific auditory cortices underlies compensatory visual functions in the deaf. Nat Neurosci. 13:1421–1427.
Mao YT, Hua TM, Pallas SL. 2011. Competition and convergence between auditory and cross-modal visual inputs to primary auditory cortical areas. J Neurophysiol. 105:1558–1573.
Matsuzaki M, Honkura N, Ellis-Davies GCR, Kasai H. 2004. Structural basis of long-term potentiation in single dendritic spines. Nature. 429:761–766.
McMullen NT, Glaser EM. 1988. Auditory cortical responses to neonatal deafening: pyramidal neuron spine loss without changes in growth or orientation. Exp Brain Res. 72:195–200.
Mei B, Niu L, Cao B, Huang D, Zhou Y. 2009. Prenatal morphine exposure alters the layer II/III pyramidal neurons morphology in lateral secondary visual cortex of juvenile rats. Synapse. 63:1154–1161.
Merabet LB, Pascual-Leone A. 2010. Neural reorganization following sensory loss: the opportunity of change. Nat Rev Neurosci. 11:44–52.
Meredith MA, Allman BL. 2012. Early hearing-impairment results in crossmodal reorganization of ferret core auditory cortex. Neural Plast. 2012:601591.
Meredith MA, Chabot N, Lomber SG. 2013. Cortico-cortical connections subserving crossmodal plasticity in auditory field of the anterior ectosylvian sulcus (FAES) in the early-deaf. Soc Neurosci Abstr. 43:4056.
Meredith MA, Clemo HR. 1989. Auditory cortical projections from the anterior ectosylvian sulcus (field AES) to the superior colliculus in cat: an anatomical and electrophysiological study. J Comp Neurol. 289:687–707.
Meredith MA, Keniston LP, Allman BL. 2012. Multisensory dysfunction accompanies crossmodal plasticity following adult hearing impairment. Neuroscience. 214:136–148.
Meredith MA, Keniston LR, Dehner LR, Clemo HR. 2006. Cross-modal projections from somatosensory area SIV to the auditory field of the anterior ecosylvian sulcus (FAES) in cat: further evidence for subthreshold forms of multisensory processing. Exp Brain Res. 72:472–484.
Meredith MA, Kryklywy J, McMillan AJ, Malhotra S, Lum-Tai R, Lomber SG. 2011. Crossmodal reorganization in the early-deaf switches sensory, but not behavioral roles of auditory cortex. Proc Natl Acad Sci USA. 108:8856–8861.
Meredith MA, Lomber SG. 2011. Somatosensory and visual crossmodal plasticity in the anterior auditory field of early-deaf cats. Hear Res. 280:38–47.
Nishimura H, Hashikawa K, Doi K, Iwaki T, Watanabe Y, Kusuoka H, Nishimura T, Kubo T. 1999. Sign language "heard" in the auditory cortex. Nature. 397:116.
Okamoto K, Nagai T, Miyawaki A, Hayashi Y. 2004. Rapid and persistent modulation of actin dynamics regulates postsynaptic reorganization underlying bidirectional plasticity. Nat Neurosci. 7:1104–1112.
Olfert ED, Cross BM, McWilliam AA. 1993. Guide to the care and use of experimental animals. Ottawa (ON): Canadian Council on Animal Care.
Oray S, Majewska A, Sur M. 2004. Dendritic spine dynamics are regulated by monocular deprivation and extracellular matrix degradation. Neuron. 44:1021–1030.
Palmer LA, Rosenquist AC, Tusa RJ. 1978. The retinotopic organization of lateral suprasylvian visual areas in the cat. J Comp Neurol. 177:237–256.
Petitto LA, Zatorre RJ, Guana K, Nikelski EJ, Dostie D, Evans AC. 2000. Speech-like cerebral activity in profoundly deaf people processing signed languages: implications for the neural basis of human language. Proc Natl Acad Sci USA. 97:13961–13966.
Purpura DP. 1974. Dendritic spine "dysgenesis" and mental retardation. Science. 186:1126–1128.
Rauschecker JP. 1995. Compensatory plasticity and sensory substitution in the cerebral cortex. Trends Neurosci. 18:36–43.
Reinoso-Suárez F. 1961. Topographischer Hirnatlas der Katz fur experimentale physiologische Untersuchungen. Darmstadt, Germany: Merck.
Roder B, Rosler F. 2004. Compensatory plasticity as a consequence of sensory loss. In: Spence C, Stein BE, editors. The Handbook of Multisensory Processes. Cambridge (MA): MIT Press, pp. 719–748.
Schachtele SJ, Losh J, Dailey ME, Green SH. 2011. Spine formation and maturation in the developing rat auditory cortex. J Comp Neurol. 519:3327–3345.
Schüz A. 1986. Comparison between the dimensions of dendritic spines in the cerebral cortex of newborn and adult guinea pigs. J Comp Neurol. 244:277–285.
Segal M. 2010. Dendritic spines, synaptic plasticity and neuronal survival: activity shapes dendritic spines to enhance neuronal viability. Eur J Neurosci. 31:2178–2184.
Sherman SM, Guillery RW. 2011. Distinct functions for direct and transthalamic corticocortical connections. J Neurophysiol. 106:1068–1077.
Stewart DL, Starr A. 1970. Absence of visually influenced cells in auditory cortex of normal and congenitally deaf cats. Exp Neurol. 28:525–528.
Stranahan AM, Khalil D, Gould E. 2007. Running induces widespread structural alterations in the hippocampus and entorhinal cortex. Hippocampus. 17:1017–1022.
Stuart G, Spruston N, Hausser M. 2008. Dendrites. New York: Oxford University Press.
Trachtenberg JT, Chen BE, Knott GW, Feng G, Sanes JR, Welker E, Svoboda K. 2002. Long-term in vivo imaging of experience-dependent synaptic plasticity in adult cortex. Nature. 420:788–794.
Valverde F. 1967. Apical dendritic spines of the visual cortex and light deprivation in the mouse. Exp Brain Res. 3:337–352.
Wong C, Chabot N, Kok MA, Lomber SG. 2014. Modified areal cartography in auditory cortex following early and late-onset deafness. Cereb Cortex. 24:1778–1792.
Xu SA, Shepherd RK, Chen Y, Clark GM. 1993. Profound hearing loss in the cat following the single co-administration of kanamycin and ethacrynic acid. Hear Res. 70:205–215.